Int. J. Multiphase Flow, Vol. 1, pp. 437–464. Pergamon Press, 1974. Printed in Great Britain.

THE EFFECT OF HYDRODYNAMIC COUPLING ON THE THINNING OF A FILM BETWEEN A DROP AND ITS HOMOPHASE

X. B. REED, JR., E. RIOLO and S. HARTLAND
Technisch-Chemisches Laboratorium, Eidgenössische Technische Hochschule, Zürich, Switzerland

(*Received* 1 *September* 1973)

Abstract—The rate of thinning of a film trapped between a drop approaching its homophase according to a model incorporating hydrodynamic coupling is dramatically different from earlier, uncoupled models. Implications for film thinning of microflows analyzed in the preceding paper are here investigated using similar analytical methods to derive a nonautonomous, nonlinear evolution equation for the film thickness which has been solved numerically under a variety of conditions after asymptotic analytical behavior has been extracted. The applied force squeezing the film, together with the initial motion in the three phases, determines the rate of film thinning in a complicated manner through the coupling parameter $R = (\rho_A\mu_A/\rho_B\mu_B)^{1/2}$. Experimental observations that normal drop circulation enhances thinning, whereas reversed drop circulation can cause thickening, are predicted theoretically for the first time. Films much more viscous than their surroundings are found to thin faster than the converse case, a conclusion at odds with off-hand intuition but substantiated experimentally; both classes of systems behave differently, often qualitatively so, from predictions of hydrodynamically decoupled systems, and in particular film thinning rates are generally faster because of less resistance to drainage, although the limit of vanishing R does recover the special case of Reynolds' model. For short times, films are shown analytically to thin more rapidly if there is initially outward film motion and normal drop circulation, but with decreasing effectiveness as R increases, in contrast to the effect of R for intermediate and longer times; if there is initially inward film motion, thickening tendencies are enhanced by reverse drop circulation but with decreasing effectiveness as R increases. These and other detailed conclusions, most predicted theoretically for the first time, are not only in qualitative agreement with experimental observations, they are in quantitative agreement with available data.

1. INTRODUCTION

In the preceding paper (Reed, Riolo & Hartland 1974) the effect of flow in the adjacent phases on drainage within a fluid film was discussed in terms of analytical solutions in the three phases. The many effects of such hydrodynamic coupling on the variation of film thickness with time are considered in the present paper, a matter of paramount importance in coalescence. In turn, coalescence has important practical implications for fields as disparate as atmospheric physics (Mason 1957) and classical unit operations in chemical engineering (Hanson 1971).

Using the microscopic solution and analytical methods similar to those employed in the previous paper, a film-thinning equation has been derived from the macroscopic equations.

This nonlinear, nonautonomous ordinary differential equation has been solved numerically for a variety of circumstances, including a range of initial film thicknesses and applied forces acting on the film. More importantly, inasmuch as the effect of hydrodynamic coupling between phases has been incorporated in the model, the role of different initial flows within the three phases has been assessed for three classes of physical systems: those in which, crudely speaking, the film is much more, comparably, and much less, viscous than its surroundings.

If the film is the more viscous phase, then thinning is more rapid than the converse case, but aside from the case of effectively infinitely viscous surroundings—in which case Reynolds' model is recovered—results differ, often dramatically, generally qualitatively, and always quantitatively, from those presuming immobile interfaces. Moreover, conclusions based upon older, decoupled models can even be opposed to those for coupled systems having clean interfaces, for not only do the physical properties of the fluid in the film affect flow there, as well as serving to determine the effective force and film dimensions, and not only must flow within the film accommodate itself to flow within the contiguous phases, but the converse holds as well, with the result that physical properties in the drop and its homophase affect not only the same overall system parameters and the flow within adjacent phases, but the boundary conditions at the interfaces which act as compatibility conditions on simultaneous motion in all three phases. Said more succinctly if less precisely, there is hydrodynamic coupling influencing flow in all three phases simultaneously, which in turn influences macroscopic behavior in a still more complicated manner.

Many qualitative predictions of the theory are novel and most have been observed experimentally and understood intuitively, if not predicted theoretically. As a further test of the theory, some available experimental results (Hartland 1967; Mackay & Mason 1963) have been satisfactorily predicted using the physical properties of the specific systems, their initial film thicknesses, and the estimated initial motions in drop, film and homophase.

2. MACROSCOPIC BALANCES AND THE FILM-THINNING EQUATION

The infamous intractability of the Navier–Stokes equations is further complicated in multi-phase problems, for the boundary conditions of continuity of velocity and viscous stress couple fluid motion across fluid interfaces, as does the pressure jump due to interfacial tension and surface curvature. The dynamics of the fluid motion are generally inextricably intertwined with the dynamics of the interface(s): the location and geometry of the boundary are neither fixed nor is their evolution in time known *a priori*, but instead they determine and are determined by the fluid motion of the contiguous phases. The crucial assumption permitting separate solution of the microflow and macroflow equations in coalescence is the quasi-static assumption, which rests firmly on the experimental fact that the final, rate-controlling stage of coalescence is drainage of a thin film of continuous phase (Mackay & Mason 1963; Reynolds 1881, 1886; Hartland 1970). The physical conditions of the drainage stage permitting simplification of the Navier–Stokes equations have already been discussed (Reed, Riolo & Hartland 1974), but the approximate uniformity in thickness does deserve

mention in the macroscopic context, for otherwise not only can the model of microflow fail, the macroflow equations can become (r, t)—partial, instead of ordinary, differential equations (Hartland 1969).

Once the drainage stage of the overall coalescence process has begun, then, the time scale for fluid motion can be presumed distinct from that for approach of the drop to its homophase through the overall quasi-static behavior of the system. The time-dependent boundaries enter microflow equations and solutions only parametrically, and the micro-solutions—obtained for arbitrary (dynamic) pressure gradients—can be used in the derivation of the film-thinning equation from the macroscopic equations. The macroscopic equations, conservation of mass in the film and balance of forces on the drop, then close the circle by determining the pressure field in the film which opposes the applied force acting on the film. The procedure is as follows.

The macroscopic balances expressing conservation of mass in the draining film and balance of forces on the drop under the stated conditions are

$$2\pi r \int_o^\delta v_r^A \, dz = \pi r^2 v \qquad [1]$$

and

$$f = 2\pi \int_o^{r_f} (p - p_f) r \, dr, \qquad [2]$$

in which v $(= -\partial\delta/\partial t)$ is the rate of approach of one interface to the other, f is the force causing that approach (usually the resultant gravitational force from the drop weight less its buoyancy, $= \Delta\rho Vg$, but more generally including an applied force (Hartland & Wood 1973)), r_f is the radius to the perimeter of the draining film, and p_f is the pressure there.

To deduce macroscopic motion from microscopic motion as expressed in the solution v_r^A ([23] of Reed, Riolo & Hartland (1974); see also [20]), it is simpler to use

$$\int_o^\delta v_r^A \, dz = \mathscr{L}^{-1}\left\{\int_o^\delta \tilde{u}_A \, dz\right\}, \qquad [3]$$

which is compatible with the quasi-static conditions. The point is that the integrations on the left are difficult, at best, those on the right simple. The price to be paid is that expansion methods paralleling but differing from those by Reed, Riolo & Hartland (1974) must be repeated.

The result of the calculation is the ordinary differential equation

$$\frac{d\delta}{dt} = -\frac{8\pi f t}{A^2 \rho_A}[\delta - 16 t^{1/2} \sum^{(3)}] - \frac{8}{3 r_f}[u_o \delta - 2(\Delta u) t^{1/2} \sum^{(1)}], \qquad [4]$$

in which $\Delta u = 2u_o - v_o^1 - v_o^2$, $A = \pi r_f^2$,

$$\sum^{(3)} = \frac{\nu_A^{1/2}}{(R+1)^2} \sum_{n=o}^{\infty} \left(\frac{R-1}{R+1}\right)^{2n} \left\{(R+1) i^3 \operatorname{erfc}\left(\frac{2n\delta}{2(\nu_A t)^{1/2}}\right)\right.$$

$$- (R - 1)i^3\text{erfc}\left(\frac{(2n + 2)\delta}{2(v_A t)^{1/2}}\right) - 2i^3\text{erfc}\left(\frac{(2n + 1)\delta}{2(v_A t)^{1/2}}\right)\Bigg\}$$

and

$$\sum^{(1)} = \frac{v_A^{1/2}}{(R + 1)^2} \sum_{n=o}^{\infty} \left(\frac{R - 1}{R + 1}\right)^{2n} \Bigg\{(R + 1)i^1\text{erfc}\left(\frac{2n\delta}{2(v_A t)^{1/2}}\right)$$
$$- (R - 1)i^1\text{erfc}\left(\frac{(2n + 2)\delta}{2(v_A t)^{1/2}}\right) - 2i^1\text{erfc}\left(\frac{(2n + 1)\delta}{2(v_A t)^{1/2}}\right)\Bigg\}.$$

Equation [4] is not only nonlinear, it is nonautonomous, as well. Analytical methods can not be used, but machine computations for ranges of the physical parameters and initial conditions have been made and are plotted in dimensionless form in figures 1–5. Equation [4] is made dimensionless in a natural manner upon inserting

$$\Delta = \delta/r_f, \quad \theta = tv_A/r_f^2, \quad F = f/\rho_A v_A^2, \quad U = u_o r_f/v_A, \quad \bar{U} = (\Delta u)r_f/v_A,$$

but the equation need not be rewritten.

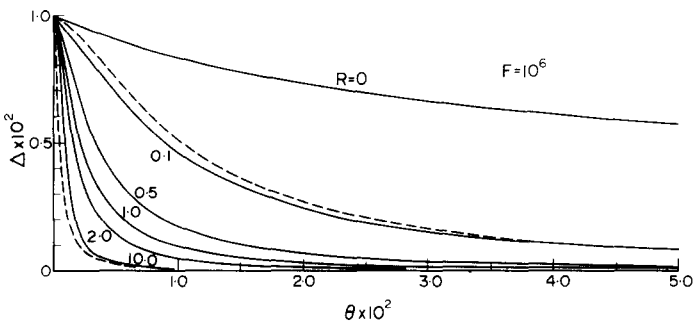

(a)

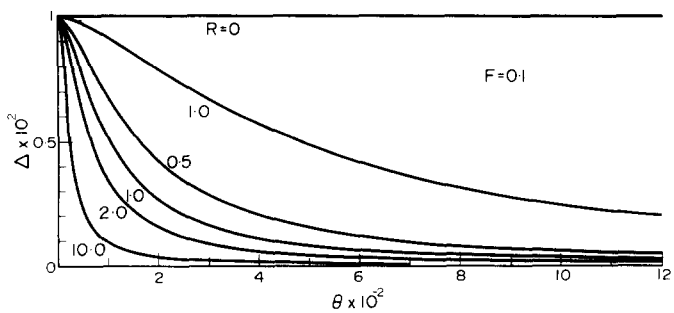

(b)

Figure 1. Effect of physical properties on film thinning for (a) $F = 10^6$, (b) $F = 0.1$.

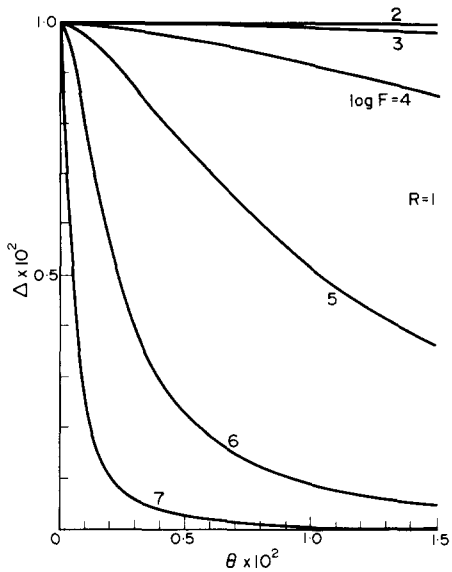

Figure 2. Effect of applied force on film thinning.

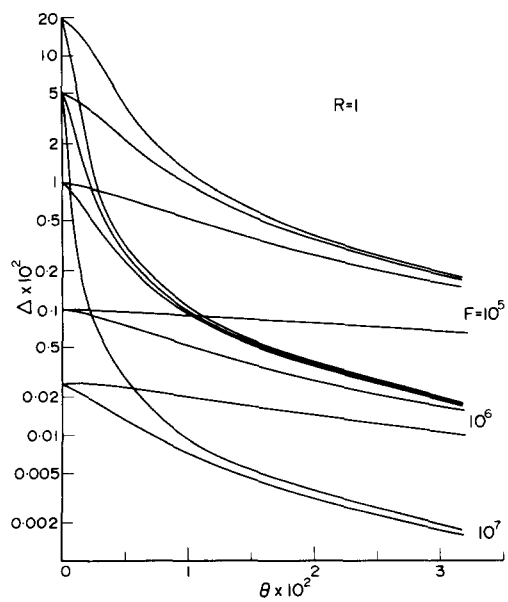

Figure 3a.

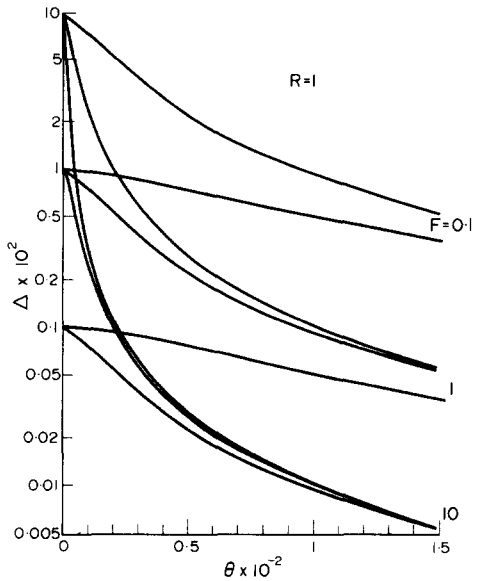

Figure 3b.

Figure 3. Effect of initial film thickness and applied force on film thinning.

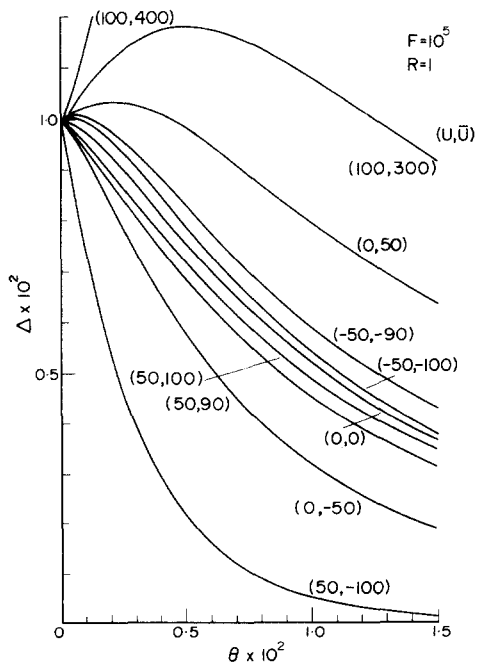

Figure 4a.

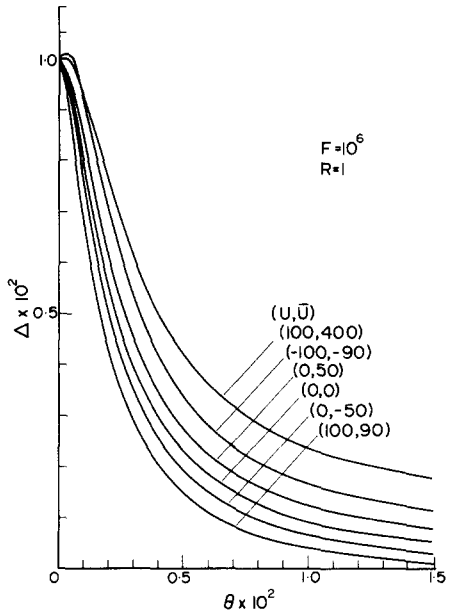

Figure 4b.

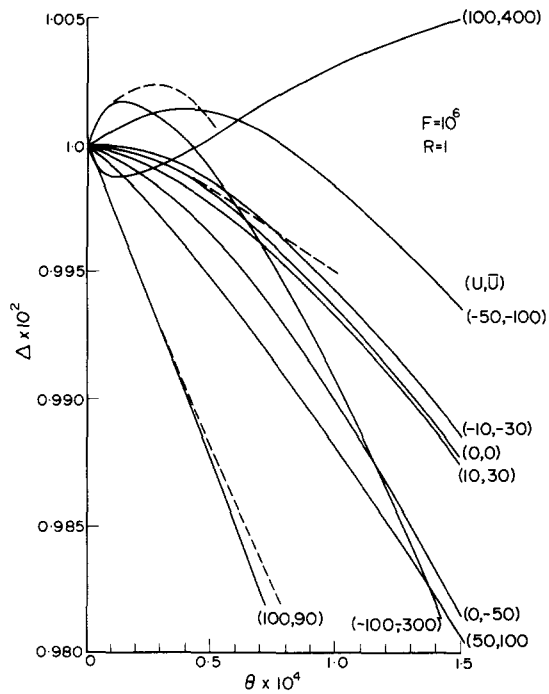

Figure 4c.

Figure 4. Effect of initial circulation patterns on film thinning.

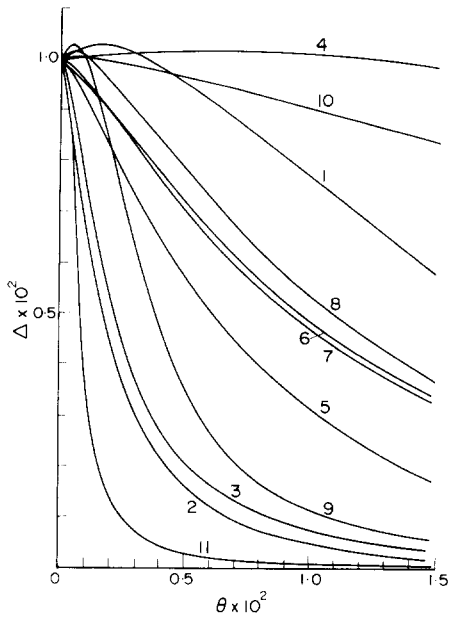

Figure 5. Interaction of the several physical effects.

Curve	R	F	U	$\bar{U}$
1	0.1	10^6	−50	−40
2	1.0	10^6	−50	−40
3	1.0	10^6	−10	−30
4	0.1	10^5	10	30
5	1.0	10^5	0	−50
6	1.0	10^5	50	100
7	0.1	10^6	−50	−100
8	1.0	10^5	−50	−100
9	10.0	10^5	−50	−100
10	0.1	10^5	−50	−100
11	10.0	10^6	−50	−100

3. ASYMPTOTIC FORMS OF THE FILM-THINNING EQUATION

The analytical intractability of the full equation lends greater import to asymptotic forms, in addition to necessitating machine computations. The solutions [23]–[25] of Reed, Riolo & Hartland (1974) for the velocity profiles converge most rapidly for short times where, unfortunately, either the microscopic–macroscopic, step-by-step decoupling procedure or the assumed initial conditions are most open to question. The short-time asymptote leads to the following differential equation,

$$\frac{\mathrm{d}\delta}{\mathrm{d}t} = -\frac{8\pi ft}{A^2\rho_A}\left[\delta - 16t^{1/2}\frac{i^3\mathrm{erfc}(o)}{(R+1)}\right] - \frac{8}{3r_f}\left[u_o\delta - 2(\Delta u)t^{1/2}\frac{i^1\mathrm{erfc}(o)}{(R+1)}\right]$$

$$= -\frac{8\pi ft}{A^2\rho_A}\left[\delta - \frac{8}{3\pi^{1/2}}\frac{t^{1/2}}{(R+1)}\right] - \frac{8}{3r_f}\left[u_o\delta - \frac{2}{\pi^{1/2}}\frac{(\Delta u)t^{1/2}}{(R+1)}\right], \quad [5]$$

which is nonautonomous although linear. If re-expressed for compactness in the dimensionless form

$$\frac{d\Delta}{d\theta} = -B(\theta)\Delta + C(\theta), \quad [6]$$

in which

$$B(\theta) = \frac{8}{3}\left[\frac{3}{\pi}F\theta + U\right]$$

$$C(\theta) = \frac{16}{3\pi^{1/2}}\frac{1}{(R+1)}\left[\left(\frac{4}{\pi}F\theta + \bar{U}\right)\right]\theta^{1/2},$$

then the general solution (see, for example, Hartman 1964; Jenson & Jeffreys 1963; Pontryagin 1962) is

$$\Delta(\theta) = \exp[-B_I(\theta)]\left[\int_o^\theta C(\tau)\exp[B_I(\tau)]\,d\tau + \Delta(o)\right], \quad [7]$$

in which

$$B_I(\theta) = \int_o^\theta B(\tau)\,d\tau = \frac{8}{3}\left[\frac{3}{2\pi}F\theta^2 + U\theta\right].$$

Table 1. Initially quiescent film.

Case 1. $U = 0$, $\bar{U} > 0$
(e.g. $v_o^1 < 0$, $u_o = v_o^2 = 0$)

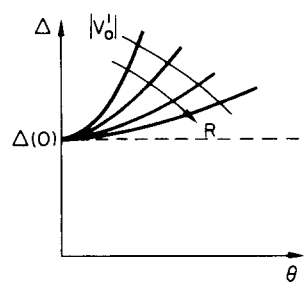

Case 2. $U = 0$, $\bar{U} < 0$
(e.g. $v_o^1 > 0$, $u_o = v_o^2 = 0$)

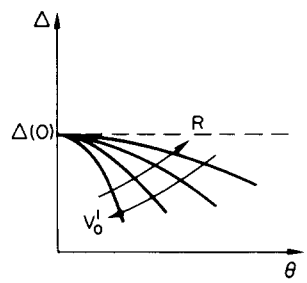

Case 3. $U = \bar{U} = 0$. Family of curves degenerates to single, initially horizontal straight line for an initially quiescent system. In all three cases other effects come into play with passage of time

Table 2. Initially outward film flow.

Case 1. $U > 0, \bar{U} > 0$
(e.g. $u_o = 0.5, v_o^1 \leq 0.9, v_o^2 = 0$)

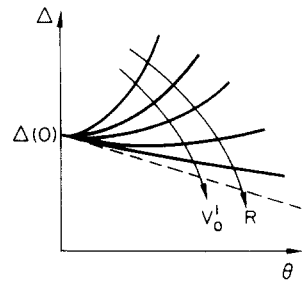

Case 2. $U > 0, \bar{U} < 0$
(e.g. $u_o = 0.1, v_o^1 > 0.2, v_o^2 = 0$)

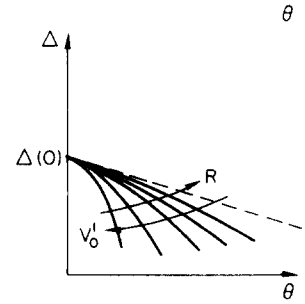

Case 3. $U < 0, \bar{U} = 0$
(e.g. $u_o = 0.5, v_o^1 = 1.0, v_o^2 = 0$)
See remark, Case 3, Table 1, but note that here the meaning of $\bar{U} = 0$ is that there is initial motion in adjacent phases corresponding to that in film

Table 3. Initially inward film flow.

Case 1. $U < 0, \bar{U} > 0$
(e.g. $u_o = -0.5, v_o^1 < -1.0, v_o^2 = 0$)

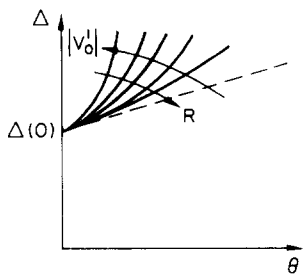

Case 2. $U < 0, \bar{U} < 0$
(e.g. $u_o = -0.5, v_o^1 = \pm 0.1, v_o^2 = 0$
or any value of v_o^1 satisfying $2u_o < v_o^1$)

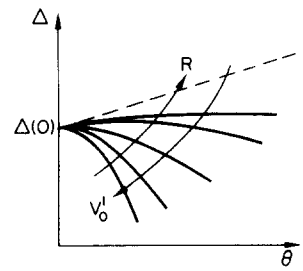

Case 3. $U < 0, \bar{U} = 0$
(e.g. $u_o = -0.5, v_o^1 = -1.0, v_o^2 = 0$)
See remarks, Cases 3, Tables 1, 2, especially 2

Table 4. Short-time behavior.

	Steady Reynolds'	Transient Reynolds'	Hydrodynamically coupled
$\frac{d\Delta}{d\theta}$	$-\frac{2}{3\pi}F\Delta^3$	$-8[F\theta/\pi + U/3]\Delta + 2\alpha[2F\theta/\pi + U]\theta^{1/2}$	$-8[F\theta/\pi + U/3]\Delta + \frac{\alpha}{R+1}[4F\theta/\pi + \bar{U}]\theta^{1/2}$
$\frac{d^2\Delta}{d\theta^2}$	$-\frac{4}{3}\left(\frac{F}{\pi}\right)^2\Delta^5$	$\alpha\left\{U\theta^{-1/2} + \frac{6}{\pi}F\theta^{1/2} - \alpha\pi^{1/2}U^2\theta^{1/2}\right.$ $\left. - \frac{5\alpha}{\pi^{1/2}}UF\theta^{3/2} - \frac{32}{\pi^2}F^2\theta^{5/2}\right\}$ $+ 8\{8[F\theta/\pi + U/3]^2 - F/\pi\}\Delta$	$\frac{\alpha}{R+1}\left\{\underline{\frac{\bar{U}}{2}\theta^{-1/2}} + \frac{6}{\pi}F\theta^{1/2} - \frac{8}{3}U\bar{U}\theta^{1/2}\right.$ $\left. - \frac{2\alpha}{\pi^{1/2}}UF\theta^{3/2} - \frac{8}{\pi}F\bar{U}\theta^{3/2} - \frac{32}{\pi^2}F^2\theta^{5/2}\right\}$ $+ 8\{8[F\theta/\pi + U/3]^2 - F/\pi\}\Delta$

Underlined terms indicate dominance for very short times: here, $\alpha = 16/3\pi^{1/2}$.

Unfortunately, the integrations are not readily carried out analytically; and although short time and exact solutions are compared for certain conditions in figure 4c but because the interplay of the several parameters can not be completely seen there nor understood from the general equation ([4]), further analysis is desirable. The results of the analysis for short times appear in tables 1–4 and are sketched in subsequent paragraphs.

The differential geometry of the trajectories in the neighborhood of the origin provides considerable information about the nature of film-thinning in hydrodynamically coupled systems, in particular, the complex interplay of the physical properties, the initial thickness and flow conditions, and the applied force. The tangent to the trajectory is $d\Delta/d\theta$, and the curvature is $d^2\Delta/d\theta^2$; a geometric interpretation of the second derivative (Morse & Feshbach 1953) is that, if $d^2\Delta/d\theta^2 < 0$, then $\Delta(\theta)$ is larger than its arithmetic average taken on either side, $[\Delta(\theta + d\theta) + \Delta(\theta - d\theta)]/2$. Upon rewriting [6] as

$$\frac{d\Delta}{d\theta} = -\frac{8}{\pi}F\theta\left(\Delta - \frac{8}{3\pi^{1/2}}\frac{\theta^{1/2}}{(R+1)}\right] - \frac{8}{3}\left[U\Delta - \frac{2}{\pi^{1/2}}\frac{\bar{U}\theta^{1/2}}{(R+1)}\right], \qquad [8]$$

the trajectory is seen to leave the origin ($\theta = 0$) horizontally if there is no initial film motion, with negative slope if there is outward motion, and with positive slope if there is inward motion, *independently* of the other parameters of the problem:

$$\frac{d\Delta}{d\theta}(\theta = 0) = -8U/3. \qquad [9]$$

These initial slopes are indicated by dashed lines in tables 1–3.

The full expression for the second derivative is more complicated, being

$$\frac{d^2\Delta}{d\theta^2} = -\frac{8}{\pi}F\left[\Delta - \frac{8}{3\pi^{1/2}(R+1)}\theta^{1/2}\right] - \frac{8}{\pi}F\theta\left[\frac{d\Delta}{d\theta} - \frac{4}{3\pi^{1/2}(R+1)}\theta^{-1/2}\right] - \frac{8}{3}\left[U\frac{d\Delta}{d\theta} - \frac{1}{\pi^{1/2}}\frac{\bar{U}\theta^{-1/2}}{(R+1)}\right], \qquad [10]$$

but for very short times it is dominated by

$$\frac{d^2\Delta}{d\theta^2} \sim 8\bar{U}/3(R+1)(\pi\theta)^{1/2}, \qquad [11]$$

which is independent of the other parameters, in particular, U: U determines the direction of the initial trajectory, but $\bar{U}$ determines its curvature. The shorter the time, the greater the initial curvature; the more viscous the film relative to its surroundings (or, the larger R is), the less is the curvature; the greater the initial flow disparity (as measured by $\bar{U}$), the greater the curvature.

The effects for short times are sketched schematically in tables 1–3 and are largely self-explanatory. It may be noted, however, that R seems to play an ambiguous role, depending solely upon the initial flows: independently of initial film motion, an increase in R enhances early stages of thinning if there is reverse drop circulation, but retards thinning if there is normal (outward) drop circulation. The physical basis for this behavior is that momentum is transferred less easily from the drop to the film, so that initially, film-thickening tendencies are retarded, as are film-thinning ones, by increasing the film viscosity relative to surroundings. Regardless of this seemingly ambivalent role during early stages of thinning, of course, increased values of R are ultimately favorable to drainage and resultant film thinning. It may also be seen from tables 1–3 that initial motion in the contiguous phases dominates that in the film for very short times, in the sense that large values of the second derivative can quickly turn the trajectory, irrespective of the initial value of the first derivative. Quantification of this last argument may be seen in [9] and [11], which may be compared in table 4 with other short-time formulae available (e.g. Hartland 1972, Riolo, Reed & Hartland 1973).

For slightly longer times, other effects come into play, necessitating consideration of equation [10]. Although only U enters the equation for $d\Delta/d\theta$, F, U and $\bar{U}$ enter the equation for $d^2\Delta/d\theta^2$ after the initial moment, as does the initial thickness $\Delta(\theta \approx 0)$. A qualitative analysis of [10] can be made, paralleling that of [11], and to that end [9] may be inserted into [10] to give

$$\frac{d^2\Delta}{d\theta^2} = \left[-\frac{8F}{\pi} + \left[\frac{8}{\pi}F\theta + \frac{8}{2}U\right]^2\right]\Delta + \frac{8}{3\pi^{1/2}}\frac{\bar{U}}{(R+1)}\theta^{-1/2}$$

$$+\left[\frac{32}{\pi^{3/2}}F - \left(\frac{8}{\pi}F\theta + \frac{8}{3}U\right)\left(\frac{16}{3\pi^{1/2}}\bar{U} + \frac{64\theta}{3\pi^{3/2}}F\right)\right]\frac{\theta^{1/2}}{(R+1)}. \qquad [12]$$

Assuming the validity of [12], we see that the first term may be positive or negative, depending upon the initial film motion and how much time has elapsed, and that the second term has already been analyzed ([11]). Consequently, a consideration of the algebraic sign of the last term, together with a balance of the magnitude of it and the other two terms yields the desired arguments concerning early trends.

A comparison with the time-dependent version of Reynolds' model (Riolo, Reed & Hartland 1973) reveals dramatic differences between even the qualitative kinds of behavior it exhibits *vis à vis* hydrodynamically coupled systems. A still sharper distinction is provided by the steady drainage model of Reynolds (Hartland 1967), for which

$$d\Delta/d\theta = -(2/3\pi)F\Delta^3 \qquad [13]$$

implies

$$d^2\Delta/d\theta^2 = -(2/\pi)^2F^2\Delta^5/3. \qquad [14]$$

The curvature is thus negative under all circumstances, the tangent inevitably downward

The physical reason for similarities between the thinning results for Reynolds' time-dependent drainage model and the present model for very short times (table 4 and below) is that the former does introduce an effect due to initial film motion (including, in particular, the possibility of initial thickening) and that the latter shows little effect of motion in the adjacent phases because only negligible motion can have been initiated for very short times. For slightly longer times, of course, these models diverge, as seen by the differences between [8] and [10] or [12] and [15] and [16], which give the differential geometry of trajectories satisfying the time-dependent Reynolds' model for short times:

$$d\Delta/d\theta = -8[(F/\pi)\theta + U/3]\Delta + 2\alpha[(2F/\pi)\theta + U]\theta^{1/2}, \qquad [15]$$

$$d^2\Delta/d\theta^2 = \alpha U\theta^{-1/2} + \frac{6\alpha}{\pi}F\theta^{1/2} - (32\alpha/\pi^2)F^2\theta^{5/2} - 5(\alpha^2/\pi^{1/2})FU\theta^{3/2}$$
$$- \alpha^2\pi^{1/2}U^2\theta^{1/2} + 8\{8[(F/\pi)\theta + U/3]^2 - F/\pi\}\Delta, \qquad [16]$$

in which $\alpha = 16/3\pi^{1/2}$.

For very short times the right side of [16] is dominated by $U\theta^{-1/2}\alpha$, precisely the result obtained for the coupled case upon setting $\overline{U} = 2U$ and passing to the limit $R \to 0$ for the above-mentioned physical reasons—and only under these very special conditions. Even for small R, in other words, there are radical differences for slightly longer times between [8] and [10] or [12] and [15] and [16], and these differences tend to become the more pronounced the longer the time. According to Reynolds' steady model, there are even nonlinear contributions to the initial curvature from the film thickness, whereas the nonlinearities are in fact in the initial flows and the force, and in interactions between these effects. Table 4 offers a ready comparison of the differential geometry of trajectories for each of the three models.

With further elapse of time, other effects come into play and invalidate the foregoing asymptotic results, the interactions between parametrically described effects becomes more complex, and only the full equation, [4], provides an adequate description. After still further elapse of time, however, the long-time asymptote will be attained:

$$\frac{d\delta}{dt} = -\frac{8\pi^{1/2}f^2}{v_A^{1/2}\rho_A A^2}t^{1/2} - \frac{4\delta}{3r_f}\left\{\frac{Ru_o\delta}{(\pi v_A t)^{1/2}} - \left[\frac{(R^2-1)\delta}{2R(\pi v_A t)^{1/2}} - 1\right](v_o^1 + v_o^2)\right\}, \qquad [17a]$$

which in dimensionless form is

$$\frac{d\Delta}{d\theta} = -\frac{8RF\Delta^2}{\pi^{3/2}}\theta^{1/2} - \frac{4\Delta}{3}\left\{\frac{R\Delta}{2(\pi\theta)^{1/2}}\overline{U} - \left[\frac{\Delta}{2R(\pi\theta)^{1/2}} + 1\right](\overline{U} - 2U)\right\}. \qquad [17b]$$

Equations [17] are analytically intractable, and their numerical solutions may be compared with those of the full equation in figure 1, where slowly thinning films are seen to be approximated reasonably well for all time, although it is longer before the asymptotic solution

actually duplicates the exact, and where duplication occurs sooner for rapidly thinning films but where the departures are much greater for shorter times (cf. dashed and solid curves of figure 1 for $R = 0.1, 10$). There is, however, an important special case of [17b] which is separable, viz., $v_o^1 = -v_o^2$, which could represent a sheared system more generally but which includes, in particular, an initially quiescent drop and homophase:

$$\frac{d\Delta}{d\theta} = -\left[\frac{8}{\pi^{3/2}} RF\theta^{1/2} - \frac{4}{3}\frac{RU}{(\pi\theta)^{1/2}}\right]\Delta^2 \qquad [18]$$

The solution of equation [18] is

$$\frac{1}{\Delta} - \frac{1}{\Delta_o} = \frac{16}{3\pi^{3/2}} RF(\theta^{3/2} - \theta_o^{3/2}) + \frac{8}{3\pi^{1/2}} RU(\theta^{1/2} - \theta_o^{1/2}). \qquad [19]$$

The asymptotic behavior for long times, in contrast to all earlier models, indicates no steady-state drainage (Reed, Riolo & Hartland 1974), regardless of the time elapsed. The simple result for thinning according to Reynolds' model (table 4) (Hartland 1967; Riolo, Reed & Hartland 1973) is not easy to compare with the more complicated long-time asymptote ([17a, b]) because they are difficult to put on a common basis and because the coupled model can have reached a specified Δ for a given F at a specified θ by any of an infinity of evolution curves, the Reynolds model but by one. Presuming the simplest of circumstances for the coupled model, namely equation [18], and taking $U = 0$ as well, thinning is inevitably more rapid according to a hydrodynamically coupled one, the ratio of the absolute values of the thinning rates being given by $(12\pi^{1/2})R\theta^{1/2}/\Delta$, a quantity taking values of 10^2–10^4 and higher for $\Delta \lesssim 10^{-2}$ and $10^{-2} < \theta < 10^2$. Thus, not only are thinning rates much higher than predicted by Reynolds' model for short and intermediate times (aside from early periods of thickening, of course) but for longer times, as well.

Two other asymptotic forms based on physical properties are important, viz., films much more and much less viscous than contiguous phases. The former corresponds to

$$\lim_{R\to\infty} \frac{d\Delta}{d\theta} = \left[\left(\frac{8F}{\pi}\right)\theta\left(\frac{16\theta^{1/2}}{R}\sum^{(3)} - \Delta\right) - \frac{8}{3}\left(U\Delta - \frac{2\bar{U}}{R}\sum^{(1)}\theta^{1/2}\right)\right]$$

$$= -8(F\theta/\pi + U/3)\Delta, \qquad [20]$$

with the series $\sum^{(3)}$ and $\sum^{(1)}$ expressed in dimensionless form; the solution of [20] is

$$\Delta(\theta)/\Delta(0) = \exp\{-8(F\theta/\pi - U/3)\theta\} \qquad [21]$$

by inspection. The latter, $R \to 0$, corresponds to

$$\lim_{R\to o} \frac{d\Delta}{d\theta} = \frac{8F}{\pi}\theta(16\theta^{1/2}\sum^{(3)} - \Delta) - \frac{8}{3}(U\Delta - 2\bar{U}\sum^{(1)}\theta^{1/2}), \qquad [22]$$

which has been treated elsewhere (Riolo, Reed & Hartland 1973). The former is plotted in figures 1a, b, showing that certainly when R is larger than 50− and generally speaking, 10− the infinite asymptote has been effectively reached. When R is smaller than 10^{-2},

correspondingly, the null asymptote has effectively been reached, as may also be seen in figures 1a, b.

The $R \to 0$ limit has significance for systems with surface active agents present, for they tend to immobilize interfacial material. The $R \to \infty$ limit also has meaning but at the opposite limit of resistance appropriate to clean interfaces in gas–liquid systems. The outright assumption of inviscid surroundings embodies little physics but does not necessarily imply an infinite rate of drainage and concomitant film thinning, as the following estimate indicates. In consequence of the lack of resistance at the film boundaries and presuming a flat initial profile and stable flow, there will also be an absence of viscous action in the film. For quasi-static motion of both film and interfaces, the microflow satisfies

$$\rho v_r \partial v_r / \partial r = -\partial p / \partial r,$$

with the macroscopic continuity equation, which yields

$$v_r = (-\mathrm{d}\delta/\mathrm{d}t) r / 2\delta,$$

and the macroscopic force balance,

$$F = \int_{r=o}^{r=r_f} [p - p(r_f)] 2\pi r \, \mathrm{d}r,$$

implying

$$\Delta(\theta)/\Delta(0) = \exp[-4(F/\pi)^{1/2}\theta], \qquad [23]$$

in dimensionless variables. This result does not have an obviously incorrect parametric dependence, for the film thins with time and more rapidly for large F. It does not, however, thin rapidly enough with the time, nor do increases in F increase the rate of thinning as much as they should, according to [21]. Both these paradoxical tendencies may be viewed as consistent with the general principle that it matters *where* in an analysis an approximation is made and that mathematical operations do *not* generally commute.

Of more practical interest is the case of comparable viscosities in both continuous and dispersed phases. The case $R = 1$, moreover, permits one to avoid a number of mathematical difficulties to obtain

$$\frac{\mathrm{d}\Delta}{\mathrm{d}\theta} = -\frac{8}{\pi} F\theta \left\{ \Delta + 4\theta^{1/2} \left[2i^3 \mathrm{erfc}\left(\frac{\Delta}{2\theta^{1/2}} \right) - \frac{1}{3\pi^{1/2}} \right] \right\}$$
$$-\frac{8}{3} \left\{ U\Delta + (\overline{U})\theta^{1/2} \left[i^1 \mathrm{erfc}\left(\frac{\Delta}{2\theta^{1/2}} \right) - \frac{1}{\pi^{1/2}} \right] \right\}, \qquad [24]$$

but the resulting simplified equation still is difficult analytically because of its nonlinearity.

4. DISCUSSION OF RESULTS

Fundamental to any broadly based or comprehensive study of coalescence is recognition of the wide variety of experimental behavior that occurs. The range, and therefore the

success, of a model must be measured by its predictions of this wealth of widely different experimental observations, both as regards qualitative processes and "events", and as regards quantitative detail and data.

The present, hydrodynamically coupled model does indeed make a variety of predictions corresponding with experimental observations. In large measure this may be traced to the several possible effects incorporated in the model, each being represented by a parameter, but it is considerably more than a matter of having additional parameters available. Rather, the basic physics underlying drainage of a thin film between a drop and its homophase have been reasonably modeled.

On the other hand, the presence of several parameters combined with the degree to which they range in nature does make exhaustive studies lengthy, as well as difficult, and their presentation prohibitive. In the following subsection concerning detailed comparisons of the theory with available quantitative experiments, an indication of the range of numerical values open to the physical parameters is given (see also tables 5a–c), justifying the selection of values used in computations. Each physical effect is thus plotted for certain values of the remaining parameters, and figures 1–5 are then not consistent, in the sense that for a given liquid pair, for instance, all manner of situations have not been investigated, nor have all manner of liquid pairs been studied in a given situation.

The special ingredient distinguishing the present model from earlier ones is the hydrodynamic coupling between motion in the film and in the drop and its homophase, and the parameter characterizing that coupling is R. It alone appears explicitly in the film-thinning equation, in contrast to v_B/v_A and R, which both appear in the microsolution, and in contrast to the total absence of other than film properties in earlier models. The effect of R on the underlying velocity profiles has already been discussed (Reed, Riolo & Hartland 1974), and its effect on the rate of film thinning is shown clearly in figures 1a, b: the more viscous

Table 5a. Values of R for various liquids relative to water at 20° C (Weast 1971).

	ρ(g/cm^3)	μ(cP)	R	R^{-1}	Ref.
Kerosene	0.813	2.4	1.40	0.72	(Perry 1963)
Benzene	0.879	0.652	0.76	1.32	(Weast 1971)
Toluene	0.867	0.590	0.72	1.39	(Weast 1971)
Chloroform	1.49	0.58	0.93	1.07	(Weast 1971)
Ether	0.714	0.233	0.41	2.44	(Weast 1971)
Dibutyl phthalate	1.048	19.2	4.48	0.22	(Mackay 1963)
Diphenyl sulfide	1.114	4.63	2.27	0.44	(Mackay 1963)
Mercury	13.59	1.54	4.57	0.22	(Weast 1971)
Liquid paraffin	0.876	140.0	11.0	0.09	(Hartland 1967)
Castor oil	0.96	986.0	30.8	0.033	(Weast 1971)
Carbon tetrachloride	1.594	0.969	1.24	0.81	(Weast 1971)
Air	0.0012	0.0018	0.0015	675.0	(Weast 1971)
Cyclohexanone*	0.946	2.01	1.29	0.77	(Weinstein 1973)
Octanol*	0.831	7.43	2.62	0.38	(Weinstein 1973)
Methylamyl acetate*	0.857	0.86	0.91	1.10	(Weinstein 1973)
Isopropyl benzene*	0.856	0.72	0.83	1.20	(Weinstein 1973)

* These values were measured after the phases had been saturated with one another (Weinstein 1973).

Table 5b. Values of R for liquids relative to glycerol at 20° C.

	R	R^{-1}
Liquid paraffin	0.25	3.95
Kerosene	0.032	31.0
Benzene	0.018	57.0
Toluene	0.017	60.2
Castor oil	0.71	1.41

Table 5c. Values of R for liquids relative to golden syrup (Hartland 1967).

	R	R^{-1}
Liquid paraffin	0.11	9.09
Kerosene	0.013	75.0
Benzene	0.0072	138.0
Toluene	0.0069	146.0
Castor oil	0.29	3.40

the film relative to its contiguous phases, the more quickly it drains (Reed, Riolo & Hartland 1974), and the more rapidly it thins. Dimensionless forces bounding those occurring in experimental and industrial practice were selected ($F = 10^{-1}, 10^{6}$), and an initially quiescent system was chosen to eliminate the effect of initial flow ($U = \overline{U} = 0$). An increase in F under these conditions shifts the family of system $-(R-)$ curves downward, but with a judicious (fortuitous) change in time scales they are remarkably similar; the dashed curves of figure 1a indicate the long-time asymptote, but there is no distinction between asymptotic and exact results for the weaker force of figure 1b.

That increases in F should not move the family of curves uniformly downward follows from the nonlinearity of the equation, but it would follow, as well, that F would generally enter the solution to even a linear equation nonlinearly. In addition to figures 1a, b, a comparison of selected curves in figures 2, 4 and 5 provides a quantitative measure of the effect of F for selected circumstances, with the modifying role of initial flows indicated in figures 4 and 5.

The considerable early effect of varying the initial film thickness $\Delta(0)$, as well as F, is shown in figures 3a, b for the base system (cf. Section 4, Reed, Riolo & Hartland 1974), emphasizing again, incidently, the nonlinearity of the problem.

A more pronounced, and indeed dramatic, effect is that of initial motion within the three phases displayed in figures 4a–c. Figure 4c has been plotted employing a different time scale to emphasize the curiosities of early stages of film thinning; asymptotic formulae [6] and [7] for short times are provided as dashed curves for comparison. Figures 4a and 4b have been separated, in turn, to show how F affects thinning for different initial conditions on the microflow. Not only is the whole family of trajectories depressed by increasing F, but in some situations where initially significant or only slight thickening occurs because of

initial reversed circulation in drop, film, and/or homophase, either slight or no thickening occurs when the applied force is increased. Consequently, the initial thickening and other phenomena arising from different initial microflows can be better seen in figure 4a than in figure 4b. For instance, reverse circulation in the drop, the film, or both ($(U, \bar{U}) = (100, 300)$, $(0, 50)$, $(-50, -90)$, $(-50, -100)$) leads to varying degrees of thickening before the inexorable action of the force squeezing the film becomes dominant. If, conversely, initial circulation patterns are outward (see especially $(50, -100)$, $(0, -50)$), then thinning is rapid from the start. The differences between thinning rates when initial circulation is inward and when it is outward are decided, but they correspond with experimental results (see, for example, Hartland 1970, 1972).

Whereas the other parameters in the film-thinning equation are well defined, initial microflows are not. The dimensionless macroscopic parameters $(U, \bar{U})$ are especially difficult to define when considered solely on the basis of the macroscopic equations. When the microscopic equations are considered, however, and when arguments are accepted, according to which comparable effects appearing in the dimensionless microscopic equations ought to have comparable orders of magnitude, then $(U, \bar{U})$ can be obtained through $u_o, v_o^1, v_o^2 \sim \pm 10^{-1} - 10^{+1}$ using $r_f/\Delta(0)$. Thus, if $u_o = 0$, 0.5 and $v_o^2 = 0$, then $v_o^1 = 0$, ± 0.1, ± 0.5 implies values such as $(U, \bar{U}) = (0, 50)$, $(50, 100)$, $(-50, -100)$, $(50, 90)$, $(-50, -90)$, etc. The parameter pair $(U, \bar{U})$ is completely defined by (u_o, v_o^1, v_o^2) if r_f and $\Delta(0)$ are known, but the converse is not true, it should be noted; to each value of $(U, \bar{U})$ there corresponds an infinity of values of (u_o, v_o^1, v_o^2).

As the collision of drops in a shear flow is practically important, for instance, yet difficult theoretically, larger values such as $(U, \bar{U}) = (100, 300)$, $(-100, -300)$ have been selected in order to get an engineering estimate of what happens in highly sheared systems which might take on values like $(u_o, v_o^1, v_o^2) = (1, -1, 0)$, $(1, -3, 2)$, $(-1, +3, -2)$, etc. to which there may correspond experimental results (Bartok & Mason 1957, 1959; Mackay & Mason 1964; Allan & Mason 1962).

Although in more viscous systems the effect is tempered, drops often deform upon impact with the homophase interface, even though the latter is itself deformable and even though an eventual conformity of the overall geometry necessarily settles in. The inertial motion of the drop causing an outer torus of its fluid to sweep downward could imply a strong reverse circulation in the drop as an initial condition for the present model, although film flow could still be outward. Under these circumstances the case $(u_o, v_o^1, v_o^2) = (1, -2, 0)$ yields $(U, \bar{U}) = (100, 400)$, the early stages of which agree well with what would be intuitively expected (figure 4c $(100, 400)$, $(-100, -300)$).

The foregoing descriptions and figures manifest most of the basic characteristics of thinning of a draining film, but by being abbreviated in number they fail to indicate the full spectrum of interactions of the several physical effects as they modulate the evolution curves. A more inclusive basis for developing physical intuition about these complex systems can be had from figure 5, where a diversity of situations appear. To be sure, they are not a complete two-dimensional representation of the multi-dimensional surface in parameter space.

Curves 1 and 2 show how sensitive trajectories are to the coupling parameter R for a system that is not initially quiescent. The reverse circulation is the same, as is the applied force, yet the film imbedded in less viscous surroundings ($R = 10$) thins rapidly and from the start, whereas the film imbedded in more viscous surroundings ($R = 0.1$) actually thickens at first.

Curve 3, which shows the effect of different initial conditions on the same system as curve 2, has been included in order that the two effects can be compared. Curve 3 may also be compared with curve 4, which shows that even though there is now outward film flow and weaker reverse drop circulation, the film initially thickens for a more extended period because the applied force is weaker.

The difference between curves 5 and 6 is the enhanced thinning that takes place if the only initial motion is outward and is in the film instead of the drop. The remaining curves 8–11 are for initially inward film flow of the same magnitude but in the presence of initially quiescent surroundings. Curves 7 and 8 have weaker overall reversed circulation than curves 1 and 2, but 8 has a brief thickening period, in contrast to 2 (both have $R = 1$), because of a weaker applied force, whereas 1 has a thickening period instead of 7 because of the reversed circulation (here, $R = 0.1$).

On the other hand, curves 6 and 7 are very similar despite large differences in every parameter. Because the surroundings for 6 are less viscous, it initially thins more rapidly (cf. [9] and [11], table 4, and associated discussion in Section 3), but in accord with the asymptotic results for long times, the larger force is the (slightly) dominant effect. Also in accord with the short and long time asymptotes, the increase in R from 8 to 9 for otherwise identical systems shows that for less viscous surroundings the film initially thickens more rapidly, but it also subsequently thins more rapidly. When curve 10 ($R = 0.1$ but otherwise identical) is brought into consideration, the difference is even more significant as initial thickening is hardly perceptible. Curves 10, 8, 9 thus provide a nice demonstration of the effect of R on otherwise identical systems in which there is initially only reverse film flow. Curves 9 and 11 show the corresponding effect of increased force for a very viscous film, with 11 thinning more rapidly than all other curves because of the larger values of R and F, and with 9 thinning more rapidly than all other systems save 2 and 3, which have an order of magnitude greater applied force; although 9 thickens more initially and although its other circumstances are less favorable to thinning than, say, 1, 5–8, because its surroundings are less viscous, its trajectory crosses theirs as it thins more rapidly.

Systems 2 and 3 thin as rapidly as 9, however, indicating comparable roles for R and F. Still more significantly, trajectories for pair 7–8 are very similar, with one having F an order of magnitude greater, the other having R an order of magnitude greater; the initial conditions are the same. Such arguments do not always transcend initial conditions, as a glance at pair 3–4 makes clear.

System 10 should, and does, thin more slowly than the others in the set 7–11, but its trajectory may also be compared with the other systems having comparable values of R, viz. 1, 4, 7. Both 1 and 7 have larger forces and thin more rapidly than 10, with 1 slower than 7 because of initially larger reversed circulation, yet 4 thins more slowly than 10 despite having an initially outward film motion because that drainage is weak and because there

is reverse drop circulation in 4 (albeit weak) and none in 10. This is also a valid generalization, although suffering the well-recognized fault of any generalization: initial motions in adjacent phases play a stronger role than comparable initial motions in films, the physical basis being the finiteness (indeed almost infinitesimalness) of the film versus the semi-infiniteness in extent of the surroundings.

The dimensionless forces of figure 5 are admittedly large. If one presumes K $(= -(\delta/v_A)^3\partial(p/\rho_A)/\partial r$, (Reed, Riolo & Hartland 1974)) ~ 1, then for films in which $\Delta(0) \sim 10^{-2}$, a value of 10^6 for F is reasonable. Such values can occur experimentally, and they do have the advantage that all scales are reduced and a variety of qualitatively distinct phenomena can be displayed in a single figure. In any event, *and despite changes in parametric interactions that can take place*, a reduction in F would yield qualitatively similar trajectories. A closer examination of even figure 5 yields more information than was described, but the foregoing nevertheless indicates the nature of the physical arguments and their associated machine computations.

The film-thinning equation, [4] offers a bit more than routine numerical difficulty. More than being nonlinear and nonautonomous, both dependent and independent variables appear as arguments of repeated integrals of complementary error functions; there are, in turn, infinite series of these mathematical functions. For typical situations the subroutine calculations of $i^n\text{erfc}(\ )$ were made to an accuracy of 10^{-8}. The convergence of the series was then confirmed using the ratio test with smallness criterion of 10^{-6}. Finally, the Runge–Kutta–Gill method provided the numerical solution, computed with an error criterion of 10^{-6}. For small values of the time, the series converge quickly because the arguments of the $i^n\text{erfc}(\ )$'s are large, regardless of n (>0). For intermediate and larger times, however, the arguments become smaller, and for an ever larger number of terms the $i^n\text{erfc}(\ )$'s are not negligible. Nevertheless, so long as R is in the neighborhood of unity, the series converge quickly because of the factor $(R - 1/R + 1)^{2n}$.

The above were mentioned for subsequent users interested in calculating $\delta(t)$ curves for specific systems, for otherwise a number of errors can enter, not all of which are so easy to recognize as a negative film thickness.

Comparison with experiment

The foregoing necessarily incomplete if somewhat systematic presentation of general film-thinning behavior in hydrodynamically coupled systems is reinforced in this subsection by a detailed comparison of specialized theoretical results with some relevant experimental results available in the literature (Hartland 1967; Mackay & Mason 1963). It is first helpful, however, to indicate the wide variety of two-phase systems occurring in nature, in industrial processes, and in laboratory research, in order to emphasize the extremes of parametric variation necessary to an exhaustive compilation of results showing the parametric dependence of film thinning in hydrodynamically coupled systems.

That kinematic viscosities of physically quite disparate fluids can be similar despite considerably wider differences of density and dynamic viscosity is a fact already emphasized in basic fluid mechanics texts (Batchelor 1970). This statement provides a useful prefatory remark, for as mentioned earlier (Reed, Riolo & Hartland 1974) it is both parameters for

each of the fluids in the two-phase system which enter the boundary-initial value problem for the underlying hydrodynamics. In fact, they enter in the special form $R = (\rho_A \mu_A / \rho_B \mu_B)^{1/2}$, and only in this form, in the film-thinning equation. If water is taken to be phase B, then $(\rho_B \mu_B)^{1/2} = 1$ g/cm^2 s$^{1/2}$, and $R = (\rho_A \mu_A)^{1/2}$, with ρ in g/cm^3 and μ in g/cm s. Conversely, if water is taken to be phase A, then $R = (\rho_B \mu_B)^{-1/2}$, using the same units. A number of fluids, most of which are immiscible in water, are tabulated in tables 5a–c. Even a superficial consideration of physical properties thus indicates a range of R from 10^{-2} to 10^{+2}. It can be wider, if gas–liquid systems of still wider property differences are selected, but the point is already made: the sensitivity of film-thinning to small changes in R is compounded by the extremely wide range of values of R that occur.

On the other hand, excepting the air–water system from table 5a for obvious fluid mechanical reasons and eliminating castor oil arbitrarily, the remaining values of R (by which we shall mean both R, R^{-1}) are roughly bounded in a definite, and significantly smaller, band: $10^{-1} < R < 10^{+1}$. The computational range of the preceding subsection was selected on the basis of this physical range of two orders of magnitude. If glycerol or golden syrup are substituted for water, then much wider ranges of R occur, but extremes of behavior due to extreme values of the physical properties cannot be modeled accurately, in general, because there can be drop deformation and oscillation of drop and homophase interfaces due to inertial effects on the one hand, or there can be such large differences in the transport properties in the two fluids that they are, in particular, not described well by a relatively simple drainage model such as ours.

The dimensionless gravitational force impressed upon the film depends upon physical parameters and drop dimensions, being given by $F = gV\Delta\rho/\rho_A v_A^2$. V can range through 10^{-1}–1 cm^3 and $\Delta\rho$ from 10^{-1} to $8 \cdot 10^{-1}$ g/cm^3, with ρ varying from 0.75 to 1.5 in liquid systems, but the greatest potential variation comes through $10^{-2} < v_A < 10^2$, roughly. Consequently, F can range from fractional values to 10^6, even in liquid–liquid systems. The situation is still worse in gas–liquid systems, despite the occurrence of smaller drops, for $\Delta\rho/\rho_A$ can easily be 10^2 or higher.

Dimensionless initial velocities can also range widely and are, moreover, more difficult to estimate in the macroscopic equations. In the microscopic equations, however, it can be argued (Reed, Riolo & Hartland 1974) that u ought not to range more than an order of magnitude or so on either side of unity, else the boundary value problem has not been made dimensionless properly, or it is not appropriate to the drainage of thin films (see also remarks in preceding subsection). For instance, although an estimate of film flow based upon flow *already existing* in a thin film between immobile interfaces could be as low as 10^{-6}, such a low value would be inconsistent with the remaining terms in the microscopic description. Worse, that would exclude the very effects which it is the purpose of the present model to describe, viz., initial and other transients occurring during drainage, on the one hand, and, on the other, those inherently inertial effects to which the model approximates despite their occurring before the drainage stage during approach or afterwards if strong reverse circulation occurs (Hartland 1970). More reasonable values of $(u_o, v_o^1, v_o^2) \sim \pm 0.1, \pm 1.0$ correspond to values in the range $U, \overline{U} \sim \pm 10^\circ - \pm 10^3$ through the factor $(\delta/r_f)^2 \sim 10^{-1} - 10^{-3}$ by which the two sets of dimensionless variables differ.

As a final precaution, it may be mentioned that the dispersion of first one, then the other, fluid of a pair does not lead to a reciprocal system, despite the fact that the values of R are reciprocals of one another. Even if drop sizes are regulated to insure the same applied force, the film properties utilized in nondimensionalizing the applied force and the time are not the same. In order to arrive at more readily comparable systems, it may be easier to employ the same fluid as continuous phase but select a pair of fluids of greater and lesser viscosity to generate (at least approximately) reciprocal values of R for equivalent dimensionless forces and time.

In figures 6–9 the theory may be compared with experimental data (solid curves) taken from the two sets of quantitative experiments available in the literature that are concerned with the approach of a drop to its homophase (Hartland 1967; Mackay & Mason 1963). Experimental thinning curves reflecting obvious asymmetries, nonuniformities and premature coalescence have been excluded, but a variety of data remain valid. The theoretical curves have not been calculated according to the exact equation ([4]), for that is expensive —especially when the parameters U and $\bar{U}$ are unknown and these dimensions of parameter space must be searched. Moreover, satisfactory to excellent results have been obtained presuming $U \neq 0$, $\bar{U} = 0$ in the long-time asymptotic formula ([17]), and hence the full calculational procedure can not be justified. The initial thickness and times are experimentally ambiguous but have not been manipulated; calculations were initiated from the raw experimental values.

For liquid paraffin films draining between golden syrup phases, $R = 0.11$. In the upper curve of figure 6, a 0.1 ml drop implying $F = 16$ shows good agreement for all but the early stages of drainage if one assumes $(U, \bar{U}) = (-0.175, 0)$. A five-fold increase in drop size —and hence F—can be predicted still more accurately if, as seems reasonable intuitively, the reverse circulation is doubled; in this case, agreement extends to the earliest stages of drainage that could be experimentally recorded.

For a 0.5 ml glycerol drop approaching its homophase through liquid paraffin, for which $R = 0.39$ and $F = 54$, no value of U such that $\bar{U} = 0$ gave better than satisfactory agreement (figure 7), but for the still larger values of R ($= 2.27$) of figure 8, good agreement was achieved. By using very small water droplets ($3.2 \cdot 10^{-4}$ cm^3) to decrease the applied force ($F = 18.7$)

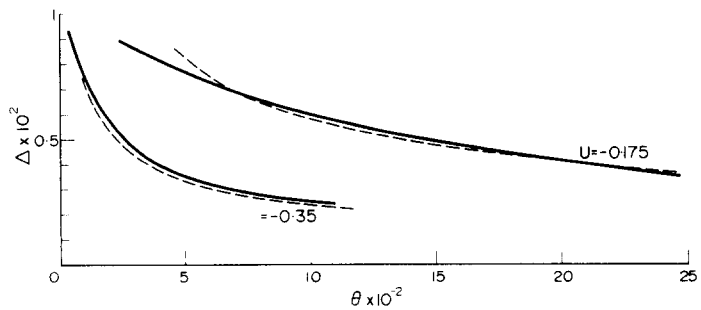

Figure 6. Comparison of theory and experiment (Hartland 1967) for $F = 16, 80$; $R = 0.11$.

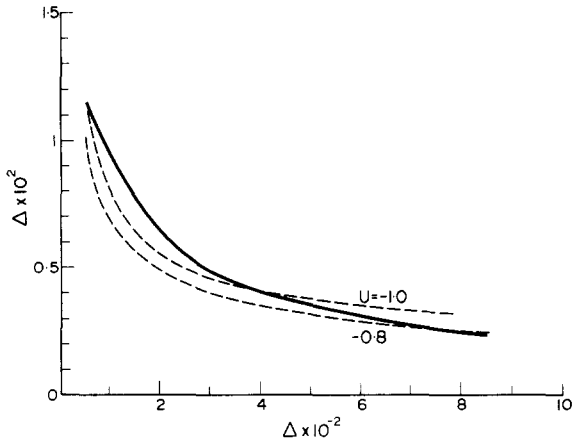

Figure 7. Comparison of theory and experiment (Hartland 1967) for $F = 54$; $R = 0.39$.

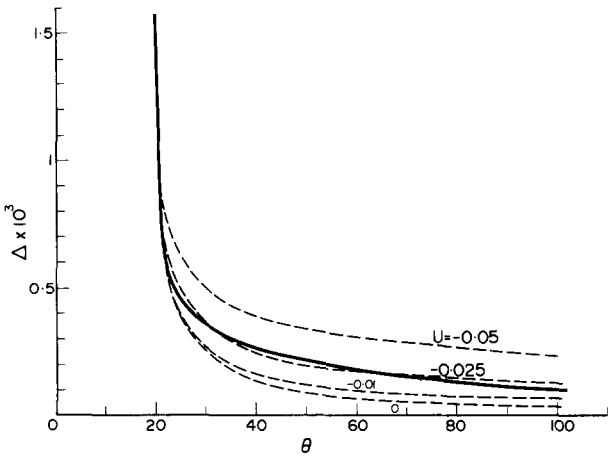

Figure 8. Comparison of theory and experiment (Mackay 1963) for $F = 18.7$; $R = 2.27$.

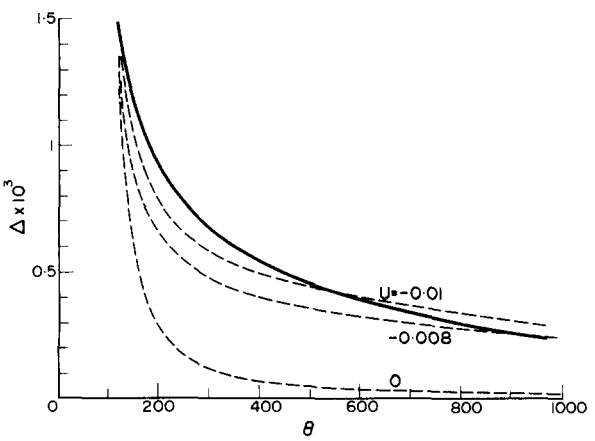

Figure 9. Comparison of theory and experiment (Mackay 1963) for $F = 0.43$; $R = 4.49$.

in the face of the decreased viscous resistance of the continuous phase of diphenyl sulfide, sufficiently low thinning rates could be experimentally recorded. The several theoretical curves indicate the relative sensitivity of even the asymptotic equation with $\bar{U} = 0$ to the rate of circulation.

The good agreement for all drainage phases of the water–diphenyl sulfide system could not be achieved if the continuous phase was made more viscous. Substituting dibutylphthalate gave an R of 4.49, and although F was only 0.43, the water–dibutylphthalate system of figure 9 only shows adequate agreement. Perhaps the remaining disparities of figures 7 and 9 could be removed by employing the exact equation and by removing the remaining experimental uncertainties—initial thickness, time, and flow in all three phases —to justify the lengthier calculational procedures, but better agreement should probably not be expected on the present basis. The excellent agreement of figures 6 and 8, however, should by no means be presumed spurious.

5. CONCLUSIONS

The present model of film-thinning is grounded in certain qualitative experimental observations—a thin, approximately uniform film that drains relatively slowly—and in the known hydrodynamic boundary conditions applicable at clean fluid–liquid interfaces which provide for hydrodynamic coupling of contiguous phases. It is not surprising, then, that this model correctly predicts a wide range of qualitative experimental observations including film thickening and enhanced film thinning due to circulation in contiguous phases, that it provides for correct dependence of thinning on physical properties in all phases, and that it agrees satisfactorily with precise quantitative experimental data for well-defined, clean systems.

Among the qualitative predictions may be included the following. Initial drainage of the film enhances film thinning, as does normal circulation in the drop. Conversely, reverse circulation in the drop or initially inward film flow causes thickening, an effect that is more pronounced the weaker the applied force. Because the volume of the drop and its homophase are virtually infinite relative to that of the film, initial motion in the drop or its homophase are more significant than initial film flow. For shorter times, initial *thickening* is less pronounced in systems having higher values of R, and yet initial *thinning* is not enhanced for increased R. Ultimately, of course, the film thins more rapidly the greater the value of R. This conclusion stands in sharp contrast to the earlier presumption growing out of Reynolds' model, according to which a reduction in film viscosity alone would lead to more rapid drainage and increased film thinning rates.

Other, more detailed, conclusions appear earlier in the article, either where derived or where computed (see especially Section 4). The most important conclusion, however, may be the most obvious one: the fact that there can be hydrodynamically coupled motion in the phases adjacent to the film at all has greater significance for drainage and film thinning than the implications of detailed situations and particular values of the parameters characterizing these newly modeled physical effects.

The quantitative predictions must be treated more carefully, for initial film thicknesses and associated initial motion in the three phases are difficult to determine experimentally and to characterize theoretically, as are film dimensions (r_f) which enter the dimensionless formulation. Nevertheless, by presuming reasonable values, a number of different physical systems for which quantitative data are available have been satisfactorily represented by the model. Extremes of parametric values do lead to difficulties, of course, as do transparently highly nonuniform or asymmetrically draining films. Moreover, films that initially thicken appreciably will generally not remain sufficiently uniform in thickness, so that quantitative agreement should not be expected in such cases.

Most of the limitations of the theory, rooted in turn in the model, are clear upon even a cursory glance, yet are all considerably more difficult to correct than to detect. The approximate uniformity of thickness and axisymmetry of drainage are easily delineated photographically. Clean interfaces are considered relatively easy to insure by modern standards of research in interfacial phenomena. In clean systems, however, the greater the density difference, the shorter the drainage period and the more inertial effects will come into play. Depending upon the surface tension, there can be strong oscillations at the interface when the drop arrives, and compounding difficulties still further would be associated—and strongly coupled—anharmonic oscillations of drop shape. By consideration of more viscous systems, inertial effects can be minimized experimentally, even though they can not readily be incorporated and analyzed theoretically. Very thick films of high curvature can not, of course, be described by the model, but the thinner the film, the less will be the effect of curvature and the more reasonable becomes the planar model.

The coupled, penetration aspect of the model and the uniformity of initial flows are the least justifiable of the assumptions. The latter can be corrected at considerable expense calculationally but with probably minimal effect practically; although easy enough in principle, the increased labor can certainly not be justified until initial flows can be accurately enough measured by as yet undesigned experiments. The semi-infinite extent of the contiguous phases, typical of engineering research, suffers obvious criticisms. In particular, it seems reasonable to conjecture that drop circulation could turn upon and reinforce both itself and film drainage, if film motion were strong enough and if the drainage stage lasted long enough, but this can be modeled only by drops which are finite in extent. Research on geometrically sounder models is under way.

Acknowledgement—We would like to thank the "Schweizerischen Nationalfonds zur Förderung der wissenschaftlichen Forschung" and the "Schweizerischen chemischen Industrie" for financial assistance.

REFERENCES

ALLAN, R. S. & MASON, S. G. 1962 Particle motions in sheared suspensions, XIV. *J. Colloid Sci.* **17**, 383–408.

BARTOK, W. & MASON, S. G. 1957 Particle motions in sheared suspensions, V. *J. Colloid Sci.* **12**, 243–262.

BARTOK, W. & MASON, S. G. 1959 Particle motions in sheared suspensions, VIII. *J. Colloid Sci.* **14**, 13.

BATCHELOR, G. K. 1970 *An Introduction to Fluid Dynamics*. Cambridge University Press.

HANSON, C. 1971 *Recent Advances in Liquid–Liquid Extraction*. Pergamon Press.

HARTLAND, S. 1967 The coalescence of a liquid drop at a liquid–liquid interface. *Trans. Inst. Chem. Engrs* **45**, t102–t108.

HARTLAND, S. 1967 The approach of a liquid drop to a flat plate. *Chem. Engng Sci.* **22**, 1675–1687.

HARTLAND, S. 1969 The profile of the draining film between a fluid drop and a deformable fluid–liquid interface. *Chem. Engng J.* **1**, 67–74.

HARTLAND, S. 1970 *The Coalescence of Liquid Drops*. British Universities Film Council.

HARTLAND, S. 1972 The effect of surface active agents on the coalescence of liquid drops. *Proc. VI. Int. Cong. Surface Activity*, Vol. 1, pp. 39–66. Zürich.

HARTLAND, S. & WOOD, S. 1973 Effect of applied force on the approach of a drop to a fluid–liquid interface. *A.I.Ch.E.J.* **19**, 871–876.

HARTMAN, P. 1964 *Ordinary Differential Equations*. Wiley.

JENSON, V. G. & JEFFREYS, G. V. 1963 *Mathematical Methods in Chemical Engineering*. Academic Press.

MACKAY, G. D. M. & MASON, S. G. 1963 The gravity approach and coalescence of fluid drops at liquid interfaces. *Can. J. Chem. Engng* **41**, 203–212.

MACKAY, G. D. M. & MASON, S. G. 1964 Particle motions in sheared suspensions, XV. *Kolloid Z.* **195**, 138–148.

MASON, B. J. 1957 *Physics of Clouds*. Oxford University Press.

MORSE, P. M. & FESHBACH, H. 1953 *Methods of Theoretical Physics*, Vol. 1, p. 6. McGraw-Hill.

PERRY, J. H. 1963 *Chemical Engineers' Handbook*. McGraw-Hill.

PONTRYAGIN, L. S. 1962 *Ordinary Differential Equations*. Addison-Wesley.

REED, X. B., RIOLO, E. & HARTLAND, S. 1974. The effect of hydrodynamic coupling on the axisymmetric drainage of thin films. *Int. J. Multiphase Flow* **1**, 411–436.

REYNOLDS, O. 1881 On drops floating on the surface of water. *Chemistry News* **44**, 211.

REYNOLDS, O. 1886 On the theory of lubrication. *Phil. Trans. R. Soc. Lond.* **A177**, 157–234.

RIOLO, E., REED, X. B. & HARTLAND, S. 1973 On initial transients in Reynolds' drainage model. *Chem. Engng J.* **6**, 121–128.

WEAST, R. C. 1971 *Handbook of Chemistry and Physics*. Chemical Rubber Co.

WEINSTEIN, B. & TREYBAL, R. E. 1973 Liquid–liquid contacting in unbaffled, agitated vessels. *A.I.Ch.E.J.* **19**, 304–312.

Sommaire—Le taux d'amincissement d'une pellicule prisonnière entre une goutte approchant son homophase selon un modèle incorporant un accouplement hydrodynamique est dramatiquement différent de celui de modèles précédents non accouplés. Les implications d'amincissement de pellicule de micro-écoulements analyses dans l'exposé précédent sont étudiées ici par des méthodes analytiques semblables pour dériver une équation d'évolution non-autonome non-linéaire pour l'épaisseur de pellicule qui a été résolue numeriquement sous une variété de conditions après

extraction du comportement analytique asymptotique. La force appliquée qui presse la pellicule ainsi que le mouvement initial dans les trois phases détermine le taux d'amincissement de pellicule de façon compliquée par le paramètre d'accouplement $R = (\rho_A\mu_A/\rho_B\mu_B)^{1/2}$. Les observations expérimentales selon lesquelles la circulation normale d'une goutte facilite l'amincissement alors que la circulation inversée d'une goutte cause l'épaississement sont théoriquement prévues pour la première fois. Les pellicules bien plus visqeuses que leur environnement s'amincissent plus rapidement que dans le cas opposé. C'est une conclusion contraire à l'intuition mais démontrée expérimentalement; les deux classes de systèmes se comportent différement, souvent de façon quantitative, selon les prédictions de systèmes hydrodynamiquement découplés, et les taux d'amincissement en particulier sont généralement plus rapides du fait de la moindre résistance au drainage, bien que la limite de disparition de R recouvre le cas spécial du modèle de Reynolds. Pour les courtes périodes, il est analytiquement montré que les pellicules s'amincissent plus rapidement s'il existe un mouvement initial vers l'extérieur de la pellicule et une circulation normale de la goutte, mais l'efficacité décroissante à mesure que R s'accroit, contrairement à l'effet de R pour les périodes intermédiaires et plus longues; s'il existe initialement un mouvement de la pellicule vers l'intérieur la tendance à l'épaississement est accrue par une circulation inversée de goutte mais avec une efficacité décroissante à mesure que R s'agrandit. Ces conclusions et d'autres détiillées, la plupart théoriquement prévues pour la première fois, ne sont pas seulement en accord qualitatif avec les observations expérimentales, mais en accord quantitatif avec les données disponibles.

Auszug—Die Abnahmegeschwindigkeit eines Films, der zwischen einem Tropfen eingeschlossen ist und welchersichseiner Homophase nähert, ist gemäß einem Modell, welches hydrodynamische Kopplung enthält, ganz bedeutend von früheren, ungekoppelten Modellen verschieden. Begleiterscheinungen für Filmabnahme von Mikroströmung, welche in dem vorangegangenen Bericht analysiert wurden, werden hier mit ähnlichen analytischen Methoden untersucht, um eine nicht autonome, nicht lineare Evolutionsgleichung für die Filmdicke abzuleiten, welche zahlenmäßig unter verschiedenen Bedingungen gelöst worden ist, nachdem asymptotisches analytisches Verhalten extrahiert worden war. Die beim Pressen des Films verwandte Kraft bestimmt zusammen mit der anfänglichen Bewegung der drei Phasen auf eine komplizierte Art durch den Kopplungsparameter $R = (\rho_A\mu_A/\rho_B\mu_B)^{1/2}$,die Geschwindigkeit der Filmabnahme. Es werden experimentelle Beobachtungen zum ersten Mal theoretisch vorausgesagt, daß normale Tropfenzirkulation abnahme steigert, während umgekehrte Tropfenzirkulation Zunahme verursachen kann. Es wird festgestellt, daß Filme, die viel viskoser als ihre Umgebung sind, schneller dünner werden, als im umgekehrten Fall, ein Schluß im Widerspruch mit spontaner, unmittelbarer Anschauung, aber experimentell begründet. Beide Systemklassen verhalten sich verschieden, oft qualitativ, aus Voraussagen von hydrodynamisch entkoppelten Systemen, und besonders sind Filmabnahme geschwindigkeiten wegen geringeren Widerstandes gegen Abfliessen des Filmes größer, obwohl die Grenze des verschwindenden R den Spezialfall des Reynolds' Modells wiedererwirkt. Es wird gezeigt, daß, analytisch, Filme für kurze Zeiten schneller dünner werden, wenn anfänglich eine Filmbewegung, nach außen gerichtet, und normale Tropfenzirkulation besteht, aber mit abnehmender Wirksamkeit bei Erhöhung von R, im Gegensatz zu der Wirkung von R für Zwischenzeiten und längere Zeiten. Wenn anfänglich Filmbewegung, nach innen gerichtet, besteht, werden Neigungen zur Zunahme durch umgekehrte Tropfenzirkulation vergrößert, jedoch mit abnehmender Wirksamkeit bei Vergrößerung von R. Diese und andere, in Einzelheiten gehende Schlüsse, welche meistens zum ersten Mal theoretisch vorausgesagt werden, stimmen nicht nur qualitativ mit experimentellen Beobachtungen überein, sondern stimmen mengenmäßig mit vorhandenen Daten überein.

Резюме—Скорость разжижения пленки уловленной между каплей, приближающейся к своей гомофазе согласно модели включающей гидродинамическое взаимодействие, очень отличается от ранних несвязанных моделей. Разжижение пленки микротечений, анализированное в предыдущей работе, исследуется здесь посредством подобных же аналитческих методов для получения неавтономного нелинейного уравнения развития толщины пленки, которое численно разрешалось при разных условиях после экстрагирования асимптотического аналитического поведения. Сила, сжимающая пленку, вместе с исходным передвижением в трех фазах, определяет степень разжижения пленки сложным способом

посредством параметра взаимодействия $R = (\rho_A \mu_A / \rho_B \mu_B)^{1/2}$. Впервые после экспериментальных наблюдений предсказано, что нормальная капельная циркуляция усиляет разжижение, в то время как обратная циркуляция капель может повести к сгущению, нашли, что пленки более вязкие, чем окружающая среда разжижаются быстрее, чем менее вязкие пленки,—заключение противоречащее интуиции, но обоснованное на экспериментах. Оба класса систем ведут себя различно, часто качественно, из предсказаний для систем с гидродинамически нарушенной связью в особенности скорости разжижения пленок происходит быстрее вследствие меньшего сопротивления свободному стеканию, хотя, предел исчезающего R спасает специальный случай модели Рейнольда. Аналитически показано, что пленки разжижаются быстрее в короткие промежутки времени, если их исходное передвижение направленно наружу и происходит нормальная капельная циркуляция, но по мере повышения R с понижающейся эффективностью, в контраст воздействию R для промежуточного и длительного времени: если же исходное передвижение пленки направлено внутрь, то тенденция к сгущению усиливается обратной циркуляцией капель, понижая эффективность и повышая R. Эти и другие детальные заключения, большинство из которых теоретически предсказано в первый раз не только качественно совпадают с экспериментальными наблюдениями, но и численно с имеющимися данными.